Phylogenetic, Structural, and Immunogenic Analysis of Algal L-Asparaginases: Potential Alternatives for ALL Treatment

Mahdis Mofidi[1], Mohammad Yaghoubi-Avini*[1]

Received: 2025-06-02 Accepted: 2025-09-01

Abstract

L-asparaginase is an essential drug used in the treatment of acute lymphoblastic leukemia (ALL), a highly prevalent cancer in children. However, its immunogenicity and allergenicity often lead to adverse reactions in patients. As a result, alternative strategies, such as identifying novel enzyme sources and employing protein engineering, have been explored. This study aimed to elucidate the molecular structure and predict the immunogenic profile of L-asparaginases from *Spirulina subsalsa*, *Nannochloropsis gaditana* CCMP526, and *Gracilaria domingensis* to propose potential substitutes for bacterial asparaginases, such as EcAII and ErAII. The corresponding enzyme sequences were retrieved from GenBank. Phylogenetic analysis revealed three distinct clusters corresponding to class 1,2, and 3 L-asparaginases. Algal enzymes from *N. gaditana* CCMP526 (GenBank ID: EWM28374.1) and *G. domingensis* (GenBank ID: KAI0567449.1) clustered within class 2 L-asparaginases, whereas *S. subsalsa* (NCBI Reference Sequence ID: WP_265263300.1) exhibited a closer evolutionary relationship with class 3 asparaginases. These findings suggest that algal asparaginases possess unique functional characteristics compared to their bacterial counterparts. Immunogenicity assessment indicated that the T-cell and B-cell epitope densities of *S. subsalsa*, *N. gaditana* CCMP526, and *G. domingensis* were comparable to those of EcAII but significantly lower than ErAII. Additionally, these algal asparaginases demonstrated lower epitope density for the *HLA-DRB1*07:01 allele, which is associated with hypersensitivity reactions, suggesting a reduced likelihood of triggering immune responses. Among the algal sources, *N. gaditana* exhibited the lowest epitope density, followed by *G. domingensis* and *S. subsalsa*. However, in the B-cell epitope analysis, *S. subsalsa* demonstrated the least potential to elicit allergenic reactions, as it contained only one allergenic epitope. Structural modeling using AlphaFold 3 predicted highly reliable three-dimensional models for the algal asparaginases.

Keywords: Algal L-asparaginase, Acute Lymphoblastic leukemia, Epitope mapping, Structural modeling, Evolutionary relationship

1-Department of Microbiology and Microbial Biotechnology, Faculty of Life Sciences and Biotechnology, Shahid Beheshti University, Tehran, Iran
*Corresponding author email address: m_yaghoubi@sbu.ac.ir
Doi: 10.48308/pae.2025.238893.1111

Introduction

L-asparaginase (ASNase) is an enzyme with industrial and therapeutic applications. It is primarily recognized for its ability to reduce acrylamide formation in the food industry and its crucial role in treating acute lymphoblastic leukemia (ALL). This enzyme is an essential component of combination chemotherapy for ALL, playing a key role in inhibiting the proliferation of asparagine-dependent cancer cells. Given the high prevalence of ALL, accounting for approximately 30% of childhood malignancies, extensive research is being conducted to identify and optimize ASNase sources from various microorganisms (Andrade et al. 2024; Belén et al. 2019). The antitumor properties of ASNase arise from the hydrolysis of L-asparagine into aspartic acid and ammonia. While healthy cells can synthesize asparagine, neoplastic cells rely on external sources for growth and survival. ASNase depletes circulating asparagine, leading to the inhibition of leukemic cells, nutrient depletion, DNA damage, cell cycle arrest, and ultimately apoptosis. This mechanism makes ASNase a key agent in chemotherapy for ALL (Pedroso et al. 2023).

Structurally, L-asparaginases are classified into three groups (Loch and Jaskolski 2021): Class 1 includes tetrameric enzymes, initially identified in bacteria but also found in yeasts and mammals (Karamitros and Konrad 2014). This class comprises cytoplasmic (Type I) enzymes that exhibit low substrate affinity (mM) and periplasmic (Type II) enzymes that demonstrate a higher affinity (μM) for L-asparagine (Srikhanta et al. 2013). Class 2 contains Type III enzymes, divided into potassium-dependent and potassium-independent proteins. These enzymes are initially inactive and acquire catalytic activity through self-maturation (Linhorst and Lübke 2022a; Loch et al. 2022). Class 3 includes Type IV (thermostable) and Type V (thermolabile) enzymes, originally identified in *Rhizobium etli*. These enzymes exist as homodimers with low substrate affinity for L-asparagine (Borek and Jaskólski 2001; Loch et al. 2023).

Currently, only Type II (Class 1) ASNases from *Escherichia coli* (EcAII) and *Erwinia chrysanthemi* (ErAII) are approved for ALL treatment (Tosta Pérez et al. 2023a). However, in addition to glutaminase activity, which contributes to severe side effects, these enzymes exhibit high immunogenicity and allergenicity, triggering adverse immune responses in patients (Belén et al. 2020). Hypersensitivity reactions associated with ASNase include anaphylaxis, bronchospasm, urticaria, itching, limb swelling, and erythema. 30–75% of patients experience hypersensitivity reactions, and up to 70% develop anti-ASNase antibodies, altering the drug's pharmacokinetics, shortening its half-life, and reducing therapeutic efficacy (Bowman et al. 2011). In some cases, this condition occurs asymptomatically while significantly diminishing drug effectiveness, known as silent inactivation (Fernandez et al. 2014; Schalk et al. 2014).

Due to these challenges, the research actively explores alternative ASNase sources with reduced immunogenicity to mitigate side effects while maintaining therapeutic efficacy. However, ASNases from Classes 2 and 3 have largely been overlooked due

to their initially perceived low substrate affinity, even though their antileukemic and immunogenic properties remaining underexplored.

This study aims to evaluate algal alternatives to bacterial ASNase using computational tools. Specifically, it focuses on the structural and immunogenic profile of ASNase derived from *Spirulina subsalsa*, *Nannochloropsis gaditana* CCMP526, and *Gracilaria domingensis*, which are economically significant algae due to their widespread applications in the food and pharmaceutical industries. These algae are recognized for their high growth rate, valuable biochemical compounds, and broad industrial utility, making them promising sources for safer and more effective therapeutic ASNase.

Material and methods

Phylogenetic Tree Reconstruction

The sequences of Class 1 (InterPro ID: IPR027474), Class 2 (InterPro ID: IPR000246), and Class 3 (InterPro ID: IPR010349) L-asparaginases (Andrade et al. 2024), along with the sequences of the three L-asparaginases studied in this research, were obtained from the InterPro database (Blum et al. 2021). Sequence alignment was performed using the MUSCLE algorithm in MEGA 7 software (Kumar, Stecher, and Tamura 2016). Then, a phylogenetic tree was constructed using the Maximum Likelihood (ML) method with the WAG+G model and 500 bootstrap replicates.

The NetMHCII 4.0 server (Kagami et al. 2020) was used to predict T-cell epitopes using default parameters. Peptides with lengths ranging from 9 to 15 amino acids were analyzed for selected alleles. The peptides were classified into three categories based on their predicted rank scores: strong binding (SB $\leq$ 1%), weak binding (WB $\leq$ 5%), and non-binding (> 5%). The epitope density was calculated using the formula fi = ni/N, where ni represents the number of predicted immunogenic epitopes (SB and WB), and N is the total number of epitopes for each allele. The alleles analyzed included HLA-DRB101:01, HLA-DRB103:01, HLA-DRB104:01, HLA-DRB107:01, HLA-DRB108:01, HLA-DRB111:01, HLA-DRB113:01 and HLA-DRB115:01.

Statistical analysis was performed utilizing Python, which included libraries such as pandas (McKinney 2010), scipy (Virtanen et al. 2020), seaborn (Waskom 2021), and matplotlib (Hunter 2007). Non-parametric methods were employed to address the potential non-normal distribution of the data. Pairwise comparisons were conducted using the Mann-Whitney U test, while the Kruskal-Wallis test was used for comparisons among multiple groups. Results, including test statistics and p-values, were considered statistically significant when $p < 0.05$. Data were presented as medians with interquartile ranges and visualized through boxplots and strip plots to illustrate the distribution of epitope densities across the different groups.

Prediction of B-cell Epitopes, Allergenicity, Antigenicity, and 3D Structure of L-Asparaginase

The topology of the outer membrane influences linear B-cell epitopes on the cell surface. To predict the linear B-cell epitopes of asparaginases from *S. subsalsa*, *N. gaditana* CCMP526, and *G. domingensis*, the AB-

CPred server (Saha and Raghava 2006a) was used. A threshold of 0.8 was applied, and the sequence length was set to 16- mers.

The allergenicity of each epitope was assessed using the AlgPred server (Saha and Raghava 2006b), while the antigenicity of these proteins was predicted using the VaxiJen server (Doytchinova and Flower 2007), with default parameters retained and tumors selected as the target organisms.

For the three-dimensional structure prediction of the enzyme, the amino acid sequences of L-asparaginase from *S. subsalsa*, *N. gaditana* CCMP526, and *G. domingensis* were input into AlphaFold 3. AlphaFold 3 is a deep learning model developed by DeepMind that predicts protein structures based on their amino acid sequences. This model provides highly accurate predictions of protein folding and spatial arrangements.

The quality of the predictions was assessed using the predicted local distance difference test (pLDDT) and predicted aligned error (PAE) metrics (Abramson et al., 2024). Finally, epitope map visualization was performed using PyMOL software (Kagami et al., 2020).

Results

Phylogenetic tree of algal L-asparaginases

The phylogenetic tree was constructed using the alignment of the L-asparaginase gene sequences from the algae *N. gaditana* CCMP526, *S. subsalsa*, and *G. domingensis*, along with 25 L-asparaginase sequences from classes 1, 2, and 3, specifically types I and II L-asparaginase. The tree (Figure 1) revealed three distinct clusters: class 3 L-asparaginases, class 2 L-asparaginases, and class 1 L-asparaginases, supported by strong bootstrap values. The cluster of class 3 L-asparaginases was distinct from class 2 enzymes, supported by a strong bootstrap value. The L-asparaginase from *S. subsalsa* was positioned within the class 3 cluster, indicating that the *S. subsalsa* enzyme shares the highest structural similarity with class 3 L-asparaginases.

The L-asparaginases from *N. gaditana* CCMP526 and *G. domingensis* were grouped within the class 2 Ntn-hydrolase family of L-asparaginases, which are mainly found in eukaryotic organisms.

Class 1 L-asparaginases were grouped into closely related branches and were distinct from the central cluster of class 2 and 3 L-asparaginases. The therapeutic asparaginases from *E. coli* and *E. chrysanthemi* were within this cluster.

Prediction of immunogenicity

Epitope density is used to evaluate the immunogenicity of proteins. It emphasizes that more epitope density is directly related to higher immunogenic potential. This concept was applied to assess the immunogenicity of asparaginases from the selected algal sources compared with clinical asparaginases from EcAII and ErAII. The results showed no significant difference in immunogenicity between the algal asparaginases and the EcAII asparaginase. However, a significant difference was observed with ErAII, which demonstrated higher immunogenicity compared to algal asparaginases and EcAII.

The algal asparaginases exhibited lower immunogenicity than clinical asparaginases, with *N. gaditana* CCMP526 showing lower immunogenicity than the others (Figure 2).

The T-cell epitope density for each of the

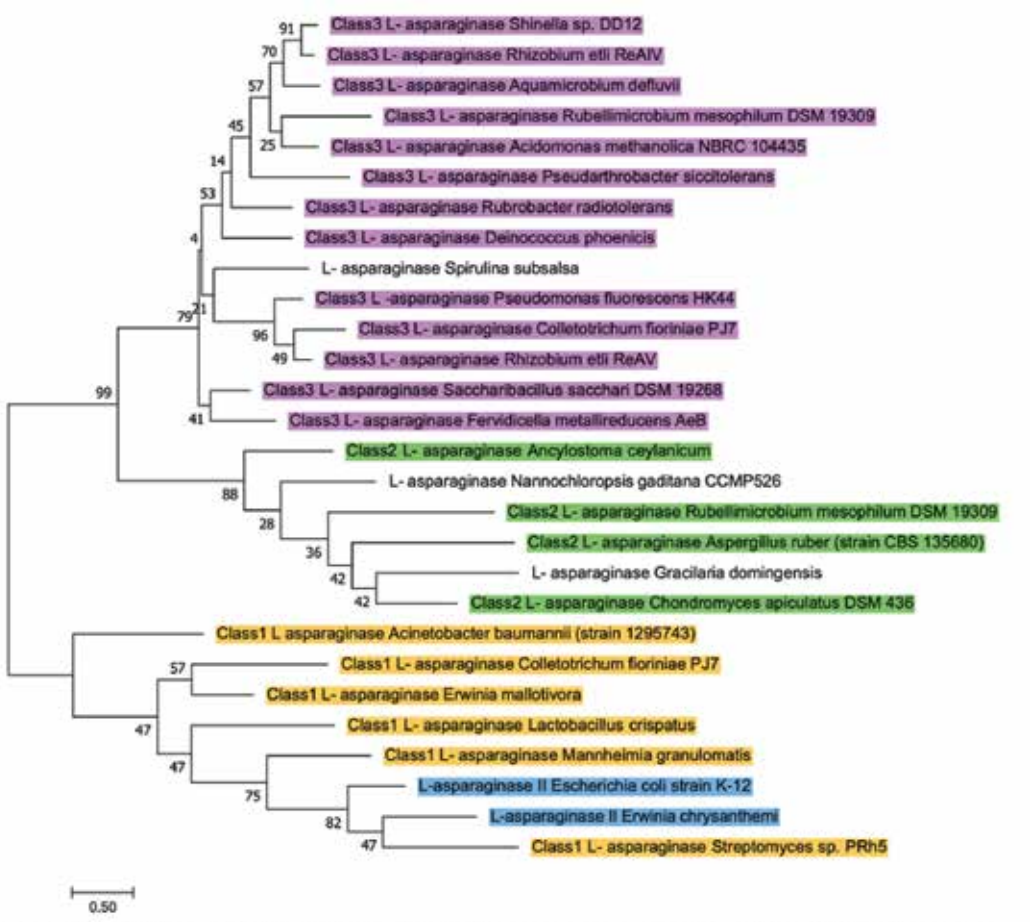

Fig. 1. The phylogenetic tree of the L-asparaginase enzyme was constructed using the maximum likelihood method and the WAG+G model. The blue color indicates microorganisms currently used in the commercial production of drugs; the classes 1, 2, and 3 are represented in yellow, green, and purple, respectively

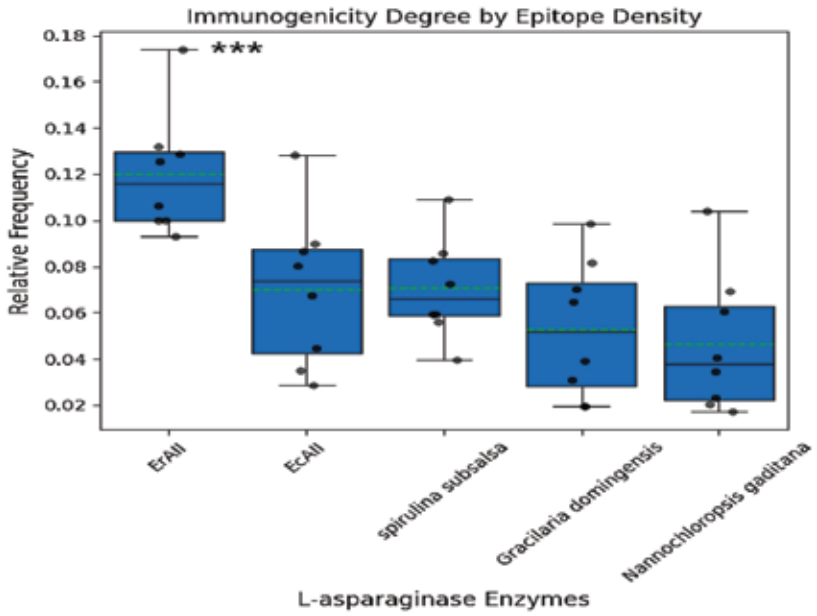

Fig. 2. Comparison of the epitope density and immunogenicity between asparaginases from *S. subsalsa*, *N. gaditana* CCMP526, *G. domingensis*, and clinical asparaginases EcAII and ErAII. The asterisk indicates the significant difference

eight (*HLA-DRB1*01:01, *HLA-DRB1*03:01, *HLA-DRB1*04:01, *HLA-DRB1*07:01, *HLA-DRB1*08:01, *HLA-DRB1*11:01, *HLA-DRB1*13:01 and *HLA-DRB1*15:01) alleles is shown in Figure 3, and the results indicate variability in distribution for each species depending on the allele. In most cases, the epitope density of *S. subsalsa*, *N. gaditana* CCMP526, and *G. domingensis* was lower than that of ErAII (Figure 3).

The HLA-DRB107:01 alleles are associated with hypersensitivity reactions and a higher risk of allergic reactions during treatment with bacterial asparaginase. The results showed that algal asparaginases exhibited lower epitope density for the HLA-DRB107:01 allele comparing EcAII and ErAII asparaginases.

Structure prediction

The AlphaFold 3 predicted the three-dimensional structure of *S. subsalsa* L-asparaginase, resulting in five structural models. The generated graphs and indicators demonstrated that the predicted structures are highly reliable. Among these structural models, the rank 1 structure was selected for its highest reliability, with a pLDDT index of approximately 100 and a PTM index of 0.96. The structures of *G. domingensis* and *N. gaditana* CCMP526 were also predicted with PTM indices of 0.84 and 0.85, respectively, indicating good structural reliability (Figure 4).

Prediction and analysis of linear B-Cell epitopes in algal asparaginases

The linear B-cell epitopes of asparaginases from *S. subsalsa*, *N. gaditana* CCMP526, and *G. domingensis* were predicted to evaluate their potential for antibody production in serum. The results revealed that *S. subsalsa* had 11 epitopes, of which one was allergenic, 10 were non-allergenic, 7 were immunogenic, and 4 were non-immunogenic. In *N. gaditana* CCMP526, 20 epitopes were identified, including 13 allergenic, 7 non-allergenic, 10 immunogenic, and 10 non-immunogenic epitopes. Similarly, *G. domingensis* exhibited 17 epitopes, with 10 allergenic, 7 non-allergen-

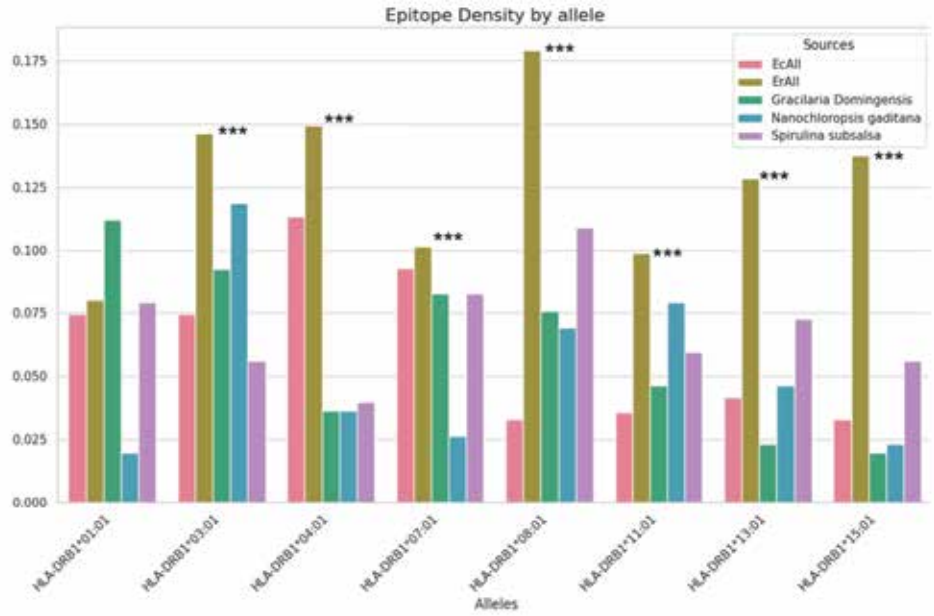

Fig. 3. The calculated epitope density for the alleles *HLA-DRB1*01:01, *HLA-DRB1*03:01, *HLA-DRB*104:01, *HLA-DRB1*07:01, *HLA-DRB1*08:01, *HLA-DRB1*11:01, *HLA-DRB1*13:01, and *HLA-DRB1*15:01 reflects the proportion of immunogenic epitopes relative to the total peptides

ic, 11 immunogenic, and 6 non-immunogenic epitopes.

The mapping of allergenic epitopes, as shown in Figure 5, indicates that most regions of *S. subsalsa* are covered by non-allergenic epitopes, making it less likely to induce hypersensitivity reactions compared to asparaginases from *N. gaditana* CCMP526 and *G. domingensis*. In contrast, *N. gaditana* CCMP526 exhibited the highest allergenic epitopes among the analyzed species, suggesting a greater potential for unwanted immune responses. Similarly, *G. domingensis* contains many allergenic and immunogenic epitopes, which may influence its immunogenic potential and likelihood of triggering immune responses.

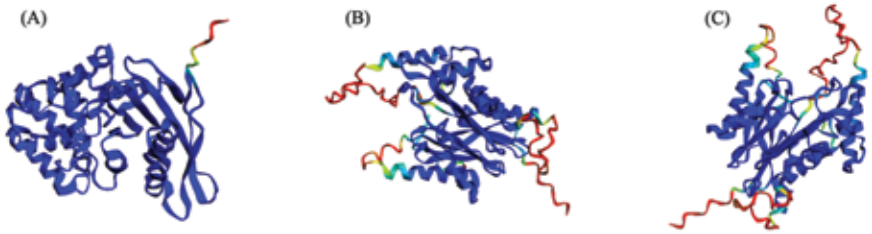

Fig. 4. Prediction of the 3D structures of asparaginases with AlphaFold 3, with colors shading from blue (high confidence) to yellow (low confidence) for each structure. Predicted enzyme structures of (A) *S. subsalsa*, (B) *G. domingensis*, and (C) *N. gaditana* CCMP526

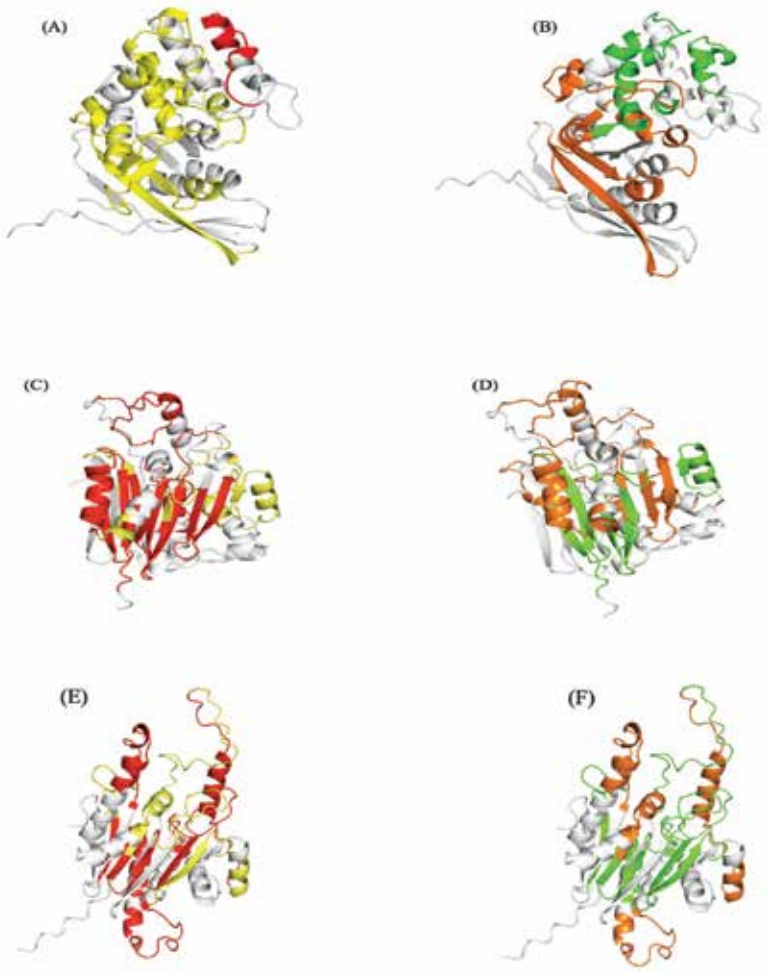

Fig. 5. Structural distribution of B-cell epitopes in the asparaginases monomers of (A, B) *S. subsalsa*; (C, D) *G. domingensis*, and (E, F) *N. gaditana* CCMP526. Panels (A, C, E) show the

Discussion

In this study, a phylogenetic tree of L-asparaginase was constructed using sequences from three algae species: *N. gaditana CCMP526*, *S. subsalsa*, and *G. domingensis*, along with 25 L-asparaginase sequences from classes 1, 2, and 3. The L-asparaginase from *S. subsalsa* was found to cluster with the L-asparaginases belonging to class 3. This class of enzymes encompassesboth permanent (thermophilic, type IV) and inducible (thermosensitive, type V) enzymes, which were initially discovered in *Rhizobium etli* (Ściuk et al. 2024). The phylogenetic tree revealed that class 3 enzymes differ significantly in amino acid sequence and structural features from the other classes. These differences are primarily attributed to unique features in their active sites and homodimeric structure. Until now, no phylogenetic studies have been conducted on the *S. subsalsa* L-asparaginase.

L-asparaginases from *N. gaditana* CCMP526 and *G. domingensis* clustered within the L-asparaginase class 2. Class 2 L-asparaginases consist of type III enzymes, which can be further divided into potassium-dependent (K-dependent) and potassium-independent (K-independent) enzymes (Sodek, Lea, and Miflin 1980). Type III L-asparaginases belong to the Ntn-hydrolase family (Linhorst and Lübke 2022b) and are produced as inactive precursors, which gain catalytic activity through self-activation.

Currently, only type II enzymes (class 1) from *E. coli* (EcAII) and *E. chrysanthemi* (ErAII) are approved for the treatment of acute lymphoblastic leukemia (ALL) (Tosta Pérez et al. 2023b). On the other hand, the potential therapeutic use of other L-asparaginases (from class 2 or class 3) has often been overlooked due to their low substrate affinity. However, recent studies have reported that class 3 L-asparaginase exhibits favorable properties and efficacy in treating ALL and AML (Ściuk et al. 2024).

This study compared the immunogenicity of L-asparaginases from *S. subsalsa*, *N. gaditana* CCMP526, and *Gracilaria domingensis* with clinical enzymes EcAII and ErAII utilizing epitope density. Epitope density measures immunogenic potential, with higher epitope densities indicating greater immune system stimulation (Belén et al. 2020). The results showed that the L-asparaginases from *S. subsalsa*, *N. gaditana* CCMP526, and *G. domingensis* exhibited immunogenicity similar to EcAII. However, significant immunogenicity was observed in ErAII, which showed a higher immunogenic potential than the other enzymes. In comparison to other algal enzymes, *N. gaditana* CCMP526 L-asparaginase showed the lowest immunogenicity. This finding suggests that some algae-derived enzymes may have better immunogenic profiles for clinical use, with *N. gaditana* demonstrating the lowest epitope density and, therefore, the least potential for unwanted immune responses.

Further analysis of T-cell epitope density revealed differences based on *HLA-DRB* alleles. Notably, the *HLA-DRB1*07:01 allele, associated with hypersensitivity reactions and an increased risk of allergic reactions during L-asparaginase treatment for leukemia (Fernandez et al. 2014), showed lower epitope density in *S. subsalsa*, *N. gaditana* CCMP526, and *G. domingensis* compared to

the clinical enzymes EcAII and ErAII. This suggests that algae-derived L-asparaginases may present a lower risk of hypersensitivity reactions. Furthermore, the type III enzyme from *N. gaditana* CCMP526 exhibits a lower allergenicity compared to other algal sources.

In addition to T-cell epitope analysis, linear B-cell epitopes were predicted to evaluate the potential for antibody production in serum. The results indicated that *S. subsalsa* had fewer allergenic epitopes than *N. gaditana* CCMP526 and *G. domingensis*, making it a safer option for clinical use. On the other hand, *N. gaditana* CCMP526 had the highest number of allergenic epitopes among the species studied, which could lead to unwanted immune responses. Moreover, *G. domingensis* displayed more allergenic epitopes and immunogenicity, which may affect its immunogenic profile and increase immune responses.

Combining the results from both T-cell and B-cell epitope analyses, it can be concluded that *S. subsalsa* represents the most appropriate candidate for clinical use. This species not only demonstrated low epitope density in both T-cell and B-cell analyses but also exhibited a reduced risk of allergic reactions, making it a safer alternative for clinical applications. In contrast, while *N. gaditana* CCMP526 exhibited the lowest T-cell epitope density, it had the highest number of allergenic epitopes in the B-cell analysis, which could potentially lead to unwanted humoral responses. *G. domingensis*, although showing some advantages over *N. gaditana*, still presented more allergenic epitopes than *S. subsalsa* and could trigger more immune reactions.

Therefore, *S. subsalsa* stands out as the most promising option for clinical use, as it offers a lower epitope density and a potentially safer immunogenic profile, with a reduced risk of triggering immune responses.

References

Abramson, Josh, Jonas Adler, Jack Dunger, Richard Evans, Tim Green, Alexander Pritzel, Olaf Ronneberger, Lindsay Willmore, Andrew J. Ballard, and Joshua Bambrick. 2024. "Accurate Structure Prediction of Biomolecular Interactions with AlphaFold 3." *Nature,* 630 (8016): 493–500.

Andrade, Kellen Cruvinel Rodrigues, Mauricio Homem-de-Mello, Julia Almeida Motta, Marina Guimarães Borges, Joel Antônio Cordeiro de Abreu, Paula Monteiro de Souza, Adalberto Pessoa, Georgios J. Pappas Jr., and e Pérola de Oliveira Magalhães. 2024. 'A Structural In Silico Analysis of the Immunogenicity of L-Asparaginase from *Penicillium Cerradense*'. *International Journal of Molecular Sciences,* 25 (9): 4788.

Belén, Lisandra Herrera, Jorge F. Beltrán Lissabet, Carlota de Oliveira Rangel-Yagui, Gisele Monteiro, Adalberto Pessoa, y Jorge, and G. Farías. 2020. 'Immunogenicity Assessment of Fungal L-Asparaginases: An in Silico Approach'. *SN Applied Sciences,* 2 (2): 222. DOI: https://doi.org/10.1007/s42452-020-2021-z.

Belén, Lisandra Herrera, Jorge Beltrán Lissabet, Carlota de Oliveira Rangel-Yagui, Brian Effer, Gisele Monteiro, Adalberto Pessoa, and Jorge G. Farías Avendaño.

2019. ‘A Structural in Silico Analysis of the Immunogenicity of L-Asparaginase from Escherichia Coli and Erwinia Carotovora’. *Biologicals,* 59:47–55.

Blum, Matthias, Hsin-Yu Chang, Sara Chuguransky, Tiago Grego, Swaathi Kandasaamy, Alex Mitchell, Gift Nuka, et al. 2021. ‘The InterPro Protein Families and Domains Database: 20 Years On’. *Nucleic Acids Research,* 49 (D1): D344–54. DOI: https://doi.org/10.1093/nar/gkaa977.

Borek, Dominika, and Mariusz Jaskólski. 2001. ‘Sequence Analysis of Enzymes with Asparaginase Activity.’ *Acta Biochimica Polonica,* 48 (4): 893–902.

Bowman, W. Paul, Eric L. Larsen, Meenakshi Devidas, Stephen B. Linda, Laurie Blach, Andrew J. Carroll, William L. Carroll, et al. 2011. ‘Augmented Therapy Improves Outcome for Pediatric High Risk Acute Lymphocytic Leukemia: Results of Children’s Oncology Group Trial P9906’. *Pediatric Blood & Cancer,* 57 (4): 569–77. DOI: https://doi.org/10.1002/pbc.22944.

Doytchinova, Irini A, and Darren R Flower. 2007. ‘VaxiJen: A Server for Prediction of Protective Antigens, Tumour Antigens and Subunit Vaccines’. *BMC Bioinformatics,* 8 (1): 4. DOI: https://doi.org/10.1186/1471-2105-8-4.

Fernandez, Christian A., Colton Smith, Wenjian Yang, Mihir Daté, Donald Bashford, Eric Larsen, W. Paul Bowman, Chengcheng Liu, Laura B. Ramsey, and Tamara Chang. 2014. ‘HLA-DRB1* 07: 01 Is Associated with a Higher Risk of Asparaginase Allergies’. *Blood, The Journal of the American Society of Hematology,* 124 (8): 1266–76.

Hunter, John D. 2007. ‘Matplotlib: A 2D Graphics Environment’. *Computing in Science & Engineering,* 9 (03): 90–95.

Kagami, Luciano Porto, Gustavo Machado das Neves, Luís Fernando Saraiva Macedo Timmers, Rafael Andrade Caceres, and Vera Lucia Eifler-Lima. 2020. ‘Geo-Measures: A PyMOL Plugin for Protein Structure Ensembles Analysis’. *Computational Biology and Chemistry* 87:107322.

Karamitros, Christos S., and Manfred Konrad. 2014. ‘Human 60-kDa Lysophospholipase Contains an N-Terminal L-Asparaginase Domain That Is Allosterically Regulated by L-Asparagine’. *Journal of Biological Chemistry,* 289 (19): 12962–75.

Kumar, Sudhir, Glen Stecher, and Koichiro Tamura. 2016. ‘MEGA7: Molecular Evolutionary Genetics Analysis Version 7.0 for Bigger Datasets’. *Molecular Biology and Evolution,* 33 (7): 1870–74. Doi: https://doi.org/10.1093/molbev/msw054.

Linhorst, Arne, and Torben Lübke. 2022a. ‘The Human Ntn-Hydrolase Superfamily: Structure, Functions and Perspectives’. *Cells,* 11 (10): 1592.

Loch, Joanna I., and Mariusz Jaskolski. 2021. ‘Structural and Biophysical Aspects of L-Asparaginases: A Growing Family with Amazing Diversity’. *IUCrJ,* 8 (4): 514–31.

Loch, Joanna I., Agnieszka Klonecka, Kinga Kądziołka, Piotr Bonarek, Jakub Barciszewski, Barbara Imiolczyk, Krzysztof Brzezinski, Mirosław Gilski, and Mariusz Jaskolski. 2022. ‘Structural and Biophysical Studies of New L-Asparaginase

Variants: Lessons from Random Mutagenesis of the Prototypic Escherichia Coli Ntn-Amidohydrolase'. *Acta Crystallographica Section D: Structural Biology,* 78 (7): 911–26.

Loch, Joanna I., Paulina Worsztynowicz, Joanna Sliwiak, Marta Grzechowiak, Barbara Imiolczyk, Kinga Pokrywka, Mateusz Chwastyk, Miroslaw Gilski, and Mariusz Jaskolski. 2023. 'Rhizobium Etli Has Two L-Asparaginases with Low Sequence Identity but Similar Structure and Catalytic Center'. *Acta Crystallographica Section D: Structural Biology,* 79 (8). Doi: https://journals.iucr.org/d/issues/2023/08/00/dw5237/dw5237.pdf.

McKinney, Wes. 2010. 'Data Structures for Statistical Computing in Python.' In *SciPy*, 445:51–56. http://conference.scipy.org.s3.amazonaws.com/proceedings/scipy2010/pdfs/mckinney.pdf.

Pedroso, Alejandro, Lisandra Herrera Belén, Jorge F. Beltrán, Rodrigo L. Castillo, Adalberto Pessoa, Enrique Pedroso, and Jorge G. Farías. 2023. 'In Silico Design of a Chimeric Humanized L-Asparaginase'. *International Journal of Molecular Sciences,* 24 (8): 7550.

Saha, Sudipto, and G. P. S. Raghava. 2006a. 'Prediction of Continuous B-cell Epitopes in an Antigen Using Recurrent Neural Network'. *Proteins: Structure, Function, and Bioinformatics,* 65 (1): 40–48. DOI: https://doi.org/10.1002/prot.21078.

Saha, Sudipto, and Gajendra Pal Singh Raghava. 2006b. 'AlgPred: Prediction of Allergenic Proteins and Mapping of IgE Epitopes'. *Nucleic Acids Research,* 34 (suppl_2): W202–9.

Schalk, Amanda M., Hien-Anh Nguyen, Coraline Rigouin, and Arnon Lavie. 2014. 'Identification and Structural Analysis of an L-Asparaginase Enzyme from Guinea Pig with Putative Tumor Cell Killing Properties'. *Journal of Biological Chemistry,* 289 (48): 33175–86.

Ściuk, Anna, Kinga Wątor, Izabela Staroń, Paulina Worsztynowicz, Kinga Pokrywka, Joanna Sliwiak, Marta Kilichowska, Kamila Pietruszewska, Zofia Mazurek, and Anna Skalniak. 2024. 'Substrate Affinity Is Not Crucial for Therapeutic L-Asparaginases: Antileukemic Activity of Novel Bacterial Enzymes'. *Molecules,* 29 (10): 2272.

Sodek, Ladaslav, Peter J. Lea, and Benjamin J. Miflin. 1980. 'Distribution and Properties of a Potassium-Dependent Asparaginase Isolated from Developing Seeds of Pisum Sativum and Other Plants'. *Plant Physiology* 65 (1): 22–26.

Srikhanta, Yogitha N., John M. Atack, Ifor R. Beacham, and Michael P. Jennings. 2013. 'Distinct Physiological Roles for the Two L-Asparaginase Isozymes of Escherichia Coli'. *Biochemical and Biophysical Research Communications,* 436 (3): 362–65.

Tosta Pérez, María, Lisandra Herrera Belén, Pablo Letelier, Yolanda Calle, Adalberto Pessoa, and Jorge G. Farías. 2023a. 'L-Asparaginase as the Gold Standard in the Treatment of Acute Lymphoblastic Leukemia: A Comprehensive Review'. *Medical Oncology,* 40 (5): 150. Doi: https://doi.org/10.1007/s12032-023-02014-9.

Virtanen, Pauli, Ralf Gommers, Travis E.

Oliphant, Matt Haberland, Tyler Reddy, David Cournapeau, Evgeni Burovski, Pearu Peterson, Warren Weckesser, and Jonathan Bright. 2020. ‘SciPy 1.0: Fundamental Algorithms for Scientific Computing in Python’. *Nature Methods,* 17 (3): 261–72.

Waskom, Michael L. 2021. ‘Seaborn: Statistical Data Visualization’. *Journal of Open Source Software,* 6 (60): 3021.